

ZnO growth on Si with low-temperature ZnO buffer layers by ECR-assisted MBE

Faxian Xiu^{a,*}, Zheng Yang^a, Dengtao Zhao^a, Jianlin Liu^a, Khan A. Alim^b,
Alexander A. Balandin^b, Mikhail E. Itkis^c, Robert C. Haddon^c

^aQuantum Structures Laboratory, Department of Electrical Engineering, University of California, Riverside, CA 92521, USA

^bNano-Device Laboratory, Department of Electrical Engineering, University of California, Riverside, CA 92521, USA

^cCenter for Nanoscale Science and Engineering, Departments of Chemistry and Chemical & Environmental Engineering, University of California, Riverside, CA 92521, USA

Received 18 February 2005; received in revised form 28 September 2005; accepted 28 September 2005

Communicated by M.S. Goorsky

Abstract

High-quality ZnO films were grown on Si(100) substrates with low-temperature (LT) ZnO buffer layers by an electron cyclotron resonance (ECR)-assisted molecular-beam epitaxy (MBE). In order to investigate the optimized buffer layer temperature, ZnO buffer layers of about 1.1 μm were grown at different growth temperatures of 350, 450 and 550 $^{\circ}\text{C}$, followed by identical high-temperature (HT) ZnO films with the thickness of 0.7 μm at 550 $^{\circ}\text{C}$. A ZnO buffer layer with a growth temperature of 450 $^{\circ}\text{C}$ (450 $^{\circ}\text{C}$ -buffer sample) was found to greatly enhance the crystalline quality of the top ZnO film compared to others. The root mean square (RMS) roughness (3.3 nm) of its surface is the smallest, compared to the 350 $^{\circ}\text{C}$ -buffer sample (6.7 nm), the 550 $^{\circ}\text{C}$ -buffer sample (7.4 nm), and the sample without a buffer layer (6.8 nm). X-ray diffraction (XRD), photoluminescence (PL) and Raman scattering measurements were carried out on these samples at room temperature (RT) in order to characterize the crystalline quality of ZnO films. The preferential c -axis orientations of (002) ZnO were observed in the XRD spectra. The full-width at half-maximum (FWHM) value of the 450 $^{\circ}\text{C}$ -buffer sample was the narrowest as 0.209 $^{\circ}$, which indicated that the ZnO film with a buffer layer grown at this temperature was better for the subsequent ZnO growth at elevated temperature of 550 $^{\circ}\text{C}$. Consistent with these results, the 450 $^{\circ}\text{C}$ -buffer sample exhibits the highest intensity and the smallest FWHM (130 meV) of the ultraviolet (UV) emission at 375 nm in the PL spectrum. The ZnO characteristic peak at 438.6 cm^{-1} was found in Raman scattering spectra for all films with buffers, which is corresponding to the E_2 mode.

© 2005 Elsevier B.V. All rights reserved.

PACS: 81.05.Dz; 81.15.Hi; 73.61.Ga

Keywords: A1. Atomic force microscopy; A1. Photoluminescence; A1. X-ray diffraction; A3. Molecular beam epitaxy; B1. ZnO buffer layer; B2. Semiconducting II–VI materials

1. Introduction

In recent years, wide band gap semiconductor, ZnO, has received considerable attention as a candidate material for optoelectronic devices such as blue light-emitting and short-wavelength laser diodes with low thresholds in the UV region [1–6]. Its unique property of a large exciton binding energy (60 meV) leads to the existence and extreme

stability of excitons at room temperature (RT) and even higher temperatures [7], which makes ZnO a highly efficient photon emitter. However, these potential applications are largely limited by the crystalline quality of ZnO epitaxial films on non-native substrates.

In most studies, sapphire has been extensively used as the substrate. But sapphire introduces complexity to device fabrication process since it is an electrically insulating material and difficult to cleave. These problems can be solved by using Si substrates. Moreover, from the viewpoint of integration with Si-based circuits and devices, the

*Corresponding author. Tel.: +1 951 827 7723; fax: +1 951 787 2425.

E-mail address: xiuf@ee.ucr.edu (F. Xiu).

growth of high-quality ZnO film on Si is of great importance. The main obstacles to get high-quality ZnO on Si, however, are to overcome the large lattice mismatch and to avoid the amorphous SiO_x layer generated at the Si surface prior to or during ZnO growth since Si can be easily oxidized in the oxygen environments [8]. To attack these problems, some efforts have been made to use ZnS [9], Zn metal layer [10], CdF_2 [11], GaN [12] and nitridation of Si surface [13]. Recently, low temperature (LT) ZnO buffer layers were reported to have remarkable improvements on the crystalline quality of ZnO by various growth techniques [14–17]. However, the optimization of buffer layers grown by MBE has not been performed, and the temperature effects of buffer layers on ZnO crystalline quality have not been reported so far.

In this paper, LT-assisted ZnO films were characterized by XRD, PL, atomic force microscopy (AFM) and Raman scattering. The optimization of growth conditions for buffer layers was reported and the growth mechanisms were analyzed.

2. Experimental procedure

ZnO films were grown on Si(100) with LT ZnO buffer layers by a Perkin-Elmer MBE system. Elemental zinc

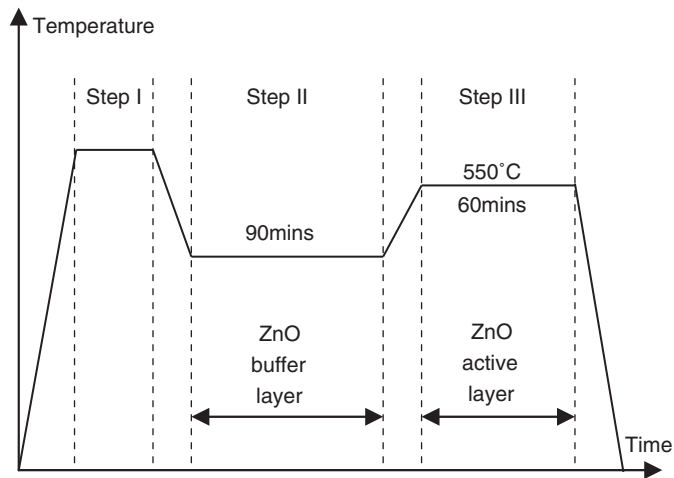


Fig. 1. ZnO on LT-ZnO/Si growth procedures: Step I, thermal cleaning process; Step II, ZnO buffer layer growth; Step III, ZnO active layer growth.

(5N) and oxygen gas (5N) were used as molecular beam sources. The zinc evaporation source was a LT effusion cell. The oxygen plasma was generated by an ECR tube. The Si substrates are (100)-oriented, n-type wafers with the resistivity of 20–30 Ωcm . All these substrates were cleaned by the Piranha–HF method and dried with nitrogen gas.

During growth, several steps were introduced as shown in Fig. 1. In step I, Si substrate was thermally cleaned at 650 °C for 10 min. In step II, ZnO buffer layers were deposited on Si at different growth temperatures of 350, 450 and 550 °C. In step III, ZnO films were grown on top of the ZnO buffer layers at 550 °C. For all these samples, the growth conditions for the top ZnO films remained the same while the growth temperatures of the buffer layers were different, as shown in Table 1. In addition, a ZnO film without a buffer layer was grown on a Si substrate at 550 °C as a comparison with the samples mentioned above.

Nanoscope III AFM was employed to observe surface morphologies. During the experiments, tapping mode was used as the scan mode. PL spectra were measured by the excitation from a 325 nm He–Cd laser at RT. PL signals were filtered by a monochromator and collected by a lock-in-amplifier. To investigate ZnO crystalline quality, Bruker Advanced D8 X-ray Diffractometer was utilized and θ – 2θ scan was performed to determine growth orientations. A Renishaw micro-Raman spectrometer 2000 with visible (488 nm) excitation lasers was used to measure Raman scattering spectra at RT.

3. Results and discussion

Surface morphologies of the ZnO films grown on Si(100) were investigated by AFM. Figs. 2(a–c) show the typical AFM images of ZnO on LT-ZnO/Si in comparison with ZnO/Si without a buffer layer (Fig. 2(d)). It is evident that all these samples show many crystal grains on the surfaces, indicating that the films were in the growth mode of the three-dimensional island. However, sample (a), which has a mediate growth temperature of 450 °C for the buffer layer, shows the relatively smaller grain size as well as a smoother surface. The RMS roughness for samples (a)–(d) are 3.3, 6.7, 7.4 and 6.8 nm, respectively. The dramatic improvement of surface roughness indicates that the growth condition for buffer layer needs to be optimized

Table 1
Growth and structural data of ZnO films

Sample	ZnO buffer layer		ZnO active layer	
	Thickness (μm)	Growth temp. ($^{\circ}\text{C}$)	Thickness (μm)	Growth temp. ($^{\circ}\text{C}$)
a	1.1	450	0.7	550
b	1.1	350	0.7	550
c	1.1	550	0.7	550
d	N/A	N/A	0.7	550

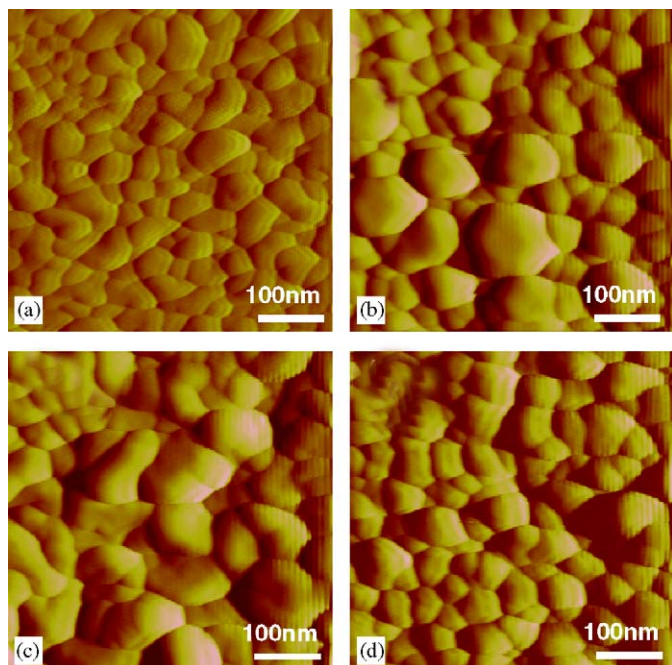


Fig. 2. AFM images of ZnO on LT-ZnO/Si: ZnO on Si with ZnO buffer layers prepared at different growth temperatures of (a) 450 °C, (b) 350 °C, and (c) 550 °C, respectively; (d) ZnO on Si without a buffer layer.

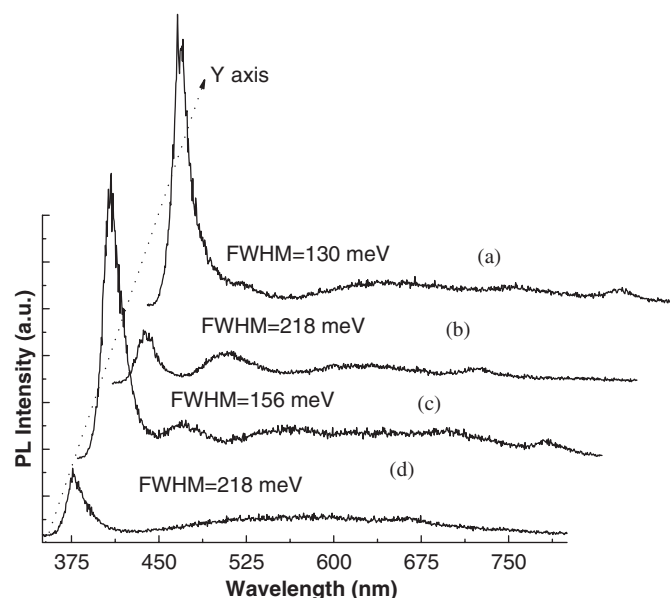


Fig. 3. RT PL spectra of samples with (a) 450 °C buffer, (b) 350 °C buffer, (c) 550 °C buffer, and (d) without a buffer layer.

to have the best effects on the surface morphology of the top ZnO film.

Figs. 3(a–d) show the RT PL spectra of ZnO on LT-ZnO/Si and ZnO/Si without a buffer layer in the wavelength range of 350–800 nm. Samples (a) and (c) show improved UV emissions compared to sample (d), peaking approximately at 376–378 nm. It was reported that ZnO shows three major luminescence emissions: an UV near-band-edge emission peaking at approximately 380 nm,

a green emission and a red emission [18]. The UV emission is due to the direct recombination of excitons or surface impurities [19]. Deep level emissions, such as green and red emissions, are closely related to structure defects, such as oxygen vacancies or zinc interstitials [20]. In our study, sample (d) shows a very broad green emission around 500 nm. Samples (b) and (c) show the pronounced emissions around 450 nm, which may be due to some unknown shallow donors or acceptors. Sample (a), with a buffer layer grown at the mediate temperature of 450 °C, however, does not show any pronounced defect-related emissions, indicating a good crystalline quality of ZnO film. The FWHM for samples (a)–(d) are 130, 218, 156 and 218 meV, respectively. These results suggest that the 450 °C-buffer film (sample (a)) has the best quality among others, which is consistent with the previous AFM analysis.

The crystal structure and orientation of ZnO films were investigated using θ - 2θ scans. Figs. 4(a–d) show the typical XRD spectra of the ZnO films prepared with and without buffer layers. It is well-known that ZnO films are usually grown with *c*-axis preferred orientation under typical growth conditions. This is because of the lowest surface energy of the (001) basal plane in ZnO, leading to a preferred growth in the (001) direction [20]. Consistent with this theory, all samples in our experiments exhibit the preferred orientation of (001), inferred from the observed (002) reflections in the XRD spectra. However, those films with buffer layers (sample (a)–(c)) show much higher diffraction intensity than the ZnO film without a buffer layer (sample (d)), which indicates the marked improvement of crystalline quality of ZnO films by employing ZnO buffer layers. Moreover, 450 °C-buffer sample (a) shows the smallest FWHM value of 0.209° as well as the highest diffraction intensity. This result has a good agreement with previous AFM and PL analysis. It is also noted that 350 °C-buffer sample (b) has another growth orientation (101). It is believed that at LT not all zinc and oxygen atoms can migrate effectively and diffuse into other crystal

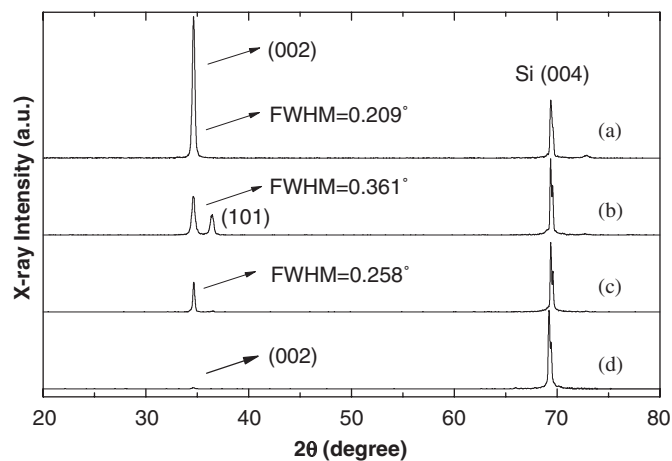


Fig. 4. XRD spectra of samples with (a) 450 °C buffer, (b) 350 °C buffer, (c) 550 °C buffer, and (d) without a buffer layer.

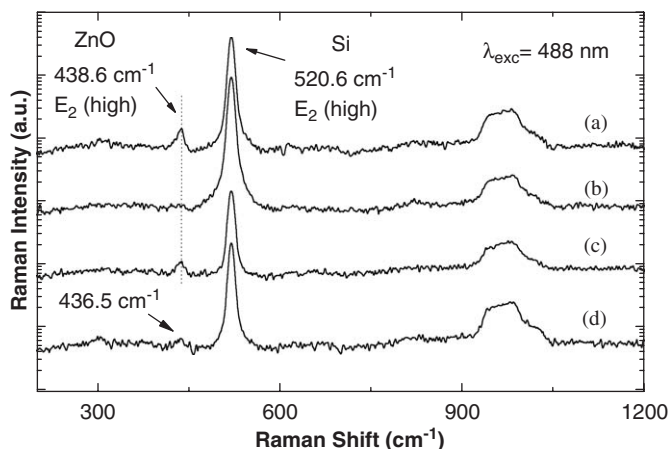


Fig. 5. Raman spectra of samples with (a) 450 °C buffer, (b) 350 °C buffer, (c) 550 °C buffer, and (d) without a buffer layer.

grains. Therefore, crystal grains with another orientation of (101) can nucleate.

Fig. 5 shows the typical Raman spectra. The ZnO characteristic peaks are observed for samples (a)–(d) at 438.6, 438.6, 438.6 and 436.5 cm^{-1} , respectively. These peaks are assigned to the vibration modes of E_2 , which are related to a band characteristic of the wurtzite phase. ZnO has a wurtzite structure and belongs to the space group C_{6v}^4 . According to group theory, there are two A_1 , two E_1 , two E_2 and two B_1 modes. Only the two B_1 modes are not Raman active. For the highly oriented ZnO films, if the incident light is perpendicular to the surface of films, only the E_2 modes and the A_1 (LO) mode are expected to observe, the other modes are forbidden according to the Raman selection rules [21]. In polycrystalline films, the frequencies of the polar LO and TO phonons can differ from the corresponding bulk ZnO crystals [22]. It was obvious that the intensity of the E_2 mode reached the highest value and FWHM is the smallest when a buffer layer was grown at 450 °C (sample (a)). Since the thickness of the ZnO films are less than the light penetration depth, E_2 (high) modes of Si substrate are observed at the frequency of 520.6 cm^{-1} , which was also reported by Ye et al. [23].

In terms of growth mechanisms, it is speculated that the quality of high temperature (HT) ZnO film depends on the quantity of threading dislocations that can penetrate the buffer layer and reach the top HT ZnO film. However, LT buffer layers can generate different amounts of point defects at different growth temperatures. These defects can interact with threading dislocations. Specifically, they can cause dislocations to climb, which helps to annihilate threading dislocation arms with opposite Burgers vectors [24]. In our experiments, at the high temperature (such as 550 °C), only a small amount of point defects are generated. The interactions between point defects and threading dislocations are so weak that most threading dislocations cannot annihilate with each other, thus easily passing through point defects and reaching the top HT

ZnO film. At the low temperature (such as 350 °C), oxygen and zinc atoms do not gain enough energy to migrate and diffuse into the neighboring area. Therefore, large-density point defects are generated and the film is isotropic. In this case, interactions between point defects and threading dislocations are negligible due to the isotropy of the buffer layer. Most threading dislocations in the buffer layer do not climb or bend, and continue to propagate to the top HT ZnO film. At the mediate temperature (such as 450 °C), however, the amount of point defects is generated in such a way that many threading dislocations strongly interact with points defects. The dislocation arms are mostly annihilated by climbing with helps from points defects. Therefore, the crystalline quality of the top HT ZnO is much better.

4. Conclusion

In summary, in order to investigate the optimized buffer layer temperature, ZnO buffer layers were grown at different growth temperatures of 350, 450 and 550 °C, followed by identical HT ZnO films at 550 °C by an ECR-assisted MBE system. Consistent results from AFM, PL, XRD, and Raman scattering demonstrate that ZnO film quality can be greatly improved by employing a LT ZnO buffer layer. For a buffer layer of about 1.1 μm , the buffer layer temperature of 450 °C was found the best condition to enhance the crystalline quality of ZnO film on top. The mechanism behind is the generation of point defects in the LT growth condition, which interact with dislocation to reduce dislocation density in the top active ZnO films.

Acknowledgements

This work was supported by DARPA/DMEA through the center for NanoScience and Innovation for Defense (CNID) under the award number H94003-04-2-0404.

References

- [1] S. Choopun, R.D. Vispute, W. Noch, A. Balsamo, R.P. Sharma, T. Venkatesan, A. Iliadis, D.C. Look, Appl. Phys. Lett. 75 (1999) 3947.
- [2] E.M. Wong, P.C. Searson, Appl. Phys. Lett. 74 (1999) 2939.
- [3] H.J. Ko, Y.F. Chen, Z. Zhu, T. Yao, I. Kobayashi, H. Uchiki, Appl. Phys. Lett. 76 (2000) 1905.
- [4] K. Ogata, K. Sakurai, Sz. Fujita, Sg. Fujita, K. Matsushige, J. Crystal Growth 214 (2000) 312.
- [5] S.J. Pearton, D.P. Norton, K. Ip, Y.W. Heo, T. Steiner, J. Vac. Sci. Technol. B 22 (2004) 932.
- [6] D.C. Look, Mater. Sci. Eng. B 80 (2001) 383.
- [7] D.C. Look, B. Clafflin, Ya.I. Alivov, S.J. Park, Phys. Stat. Sol. (A) 201 (2004) 2203.
- [8] M. Fujita, N. Kawamoto, M. Sasajima, Y. Horikoshi, J. Vac. Sci. Technol. B 22 (2004) 1484.
- [9] A. Miyake, H. Kominami, H. Tatsuoka, H. Kuwabara, Y. Nakanishi, Y. Hatanaka, J. Crystal Growth 214/215 (2000) 294.
- [10] N. Kawamoto, M. Fujita, T. Tatsumi, Y. Horikoshi, Jpn. J. Appl. Phys. 42 (2003) 7209.

- [11] M. Watanabe, Y. Maeda, S.I. Okano, *Jpn. J. Appl. Lett.* 39 (2000) L500.
- [12] A. Nahhas, H.K. Kim, J. Blachere, *Appl. Phys. Lett.* 78 (2001) 1511.
- [13] K. Iwata, P. Fons, S. Niki, A. Yamada, K. Matsubara, K. Nakahara, T. Tanabe, H. Takasu, *J. Crystal Growth* 214/215 (2000) 50.
- [14] D.Y. Lee, C.H. Choi, S.H. Kim, *J. Crystal Growth* 268 (2004) 184.
- [15] T. Nakamura, Y. Yamada, T. Kusumori, H. Minoura, H. Muto, *Thin Solid Films* 411 (2002) 60.
- [16] K. Ogata, T. Kawanishi, K. Maejima, K. Sakurai, Sz. Fujita, Sg. Fugita, *J. Crystal Growth* 237 (2002) 553.
- [17] S.H. Jeong, I.S. Kim, J.K. Kim, B.T. Lee, *J. Crystal Growth* 264 (2004) 327.
- [18] S. Cho, J. Ma, Y. Kim, Y. Sun, G.K.L. Wong, J.B. Ketterson, *Appl. Phys. Lett.* 75 (1999) 2761.
- [19] V.A. Fonoberov, A.A. Balandin, *Appl. Phys. Lett.* 85 (2004) 5971.
- [20] S.S. Kim, B.T. Lee, *Thin Solid Films* 446 (2004) 307.
- [21] Z.C. Zhang, B.B. Huang, Y.Q. Yu, D.L. Cui, *Mater. Sci. Eng. B* 86 (2001) 109.
- [22] K.A. Alim, V.A. Fonoberov, A.A. Balandin, *Appl. Phys. Lett.* 86 (2005) 053103.
- [23] J.D. Ye, S.L. Gu, S.M. Zhu, T. Chen, W. Liu, F. Qin, L.Q. Hu, R. Zhang, Y. Shi, Y.D. Zheng, *J. Vac. Sci. Technol. A* 21 (2003) 979.
- [24] E. Kasper, K. Lyutovich, M. Bauer, M. Oehme, *Thin Solid Films* 336 (1998) 319.